PALS – Setup optimisation and application to macromolecular materials characterisation

Luísa Nunes Baptista[1]

[1] *Instituto Superior Técnico, Universidade de Lisboa, Av. Rovisco Pais, 1049-001 Lisboa, Portugal*

One of the fundamental structural aspects in matter is the free volumes that exist inside materials, such as atomic defects, vacancies, voids or pores, which by enabling molecular reorganisation, strongly influence various material's macroscopic physical, chemical and mechanical properties. Positron Annihilation Lifetime Spectroscopy (PALS) is a powerful and versatile non-destructive nuclear spectroscopy technique that enables a complete study of the free volume structure inside materials, regarding the free volumes' existence, dimension and concentration, by measuring the elapsed time between the implantation of positrons into a material and the emission of the radiation resultant from the positron-electron annihilations. Given the tremendous potential of this technique, a PALS spectrometer was assembled at the Radiation, Elements and Isotopes Group (GREI) facilities to be implemented in the study of macromolecular materials developed by the research group. Before this analysis was possible, our work, consisting of a careful calibration and optimisation of the spectrometer and the development and training in essential data acquisition and analysis tools was required. Moreover, the performance of the spectrometer was evaluated through some positron lifetime measurements with appropriate standard samples of nickel, copper, electronic-grade silicon, Teflon® and polycarbonate. The obtained results were in excellent agreement with reported literature values, thus validating the system's operation and data analysis procedure. Following these successful applications, the spectrometer was employed to the study of a batch of polymeric samples fabricated by the group as a first demonstration of the usefulness of PALS on the development and study of macromolecular materials produced by GREI.

Keywords: Positron lifetime spectroscopy, Positron annihilation, Lifetime spectrometer optimisation, Timing resolution, Lifetime spectra analysis, Positron annihilation in polymers

I. INTRODUCTION

One of the techniques that is currently well-recognised for the evaluation of the micro to sub-nanometer free volume structures that exist inside matter and that are so influential on a material's physical, chemical and mechanical properties, such as viscosity, physical aging and permeability is Positron Annihilation Lifetime Spectroscopy or PALS. PALS was developed in the 1960s as part of the broad field of Positron Annihilation Spectroscopy, which encompasses a series of non-destructive nuclear spectroscopy techniques, with each exploiting a particular facet of the process of positron-electron annihilations in matter. In the case of PALS, the elapsed time between the implantation of positrons into a material and the emission of the gamma radiation resultant from these annihilations is measured. This lifetime is then used to determine the free volumes' size, concentration and distribution inside the material and relate this information with some of the material's important macroscopic features and with that evaluate their performance and suitableness for the intended applications. Despite its rich history, PALS is still a developing technique, experiencing improvements and a growing interest from many industries and technologically important areas of research. This is easily understood by the great advantages presented by PALS: it is a non-destructive technique, allowing subsequent use of the examined samples; it provides a thorough study of the material's free volumes, in a wide range of temperatures; it can probe both near-surface and in-depth regions; and the experimental setup can operate unattended and for long periods of time.

Given the tremendous potential of the PALS technique, the research group GREI - Radiation, Elements and Isotopes Group has assembled a PALS instrumental setup. This was done with the purpose of analysing a variety of polymer-based and hybrid materials synthesised by the group for biomedical and cultural heritage artefacts conservation purposes, since their free volume structure can strongly influence some critical aspects that are decisive for their performance and suitableness. However, before the spectrometer could be properly applied for these measurements, a much needed calibration and optimisation of the experimental setup was performed, mainly by revising and improving the associated electronic system. This process was backed up by the acquisition of experimental PALS spectra with the apparatus for reference materials with well known behaviour and subsequent comparison of the positron lifetime results obtained with reported literature data as well as by the development of a set of tools essential for the analysis of the acquired spectra and the transformation of the results into information regarding the analysed sample's free volumes. Finally, as a first demonstration of the spectrometer's abilities, it was applied to analysis of spectra of a series of polymeric materials developed by the research group, in order to analyse important morphological and structural characteristics of these materials.

II. POSITRON INTERACTIONS WITH MATTER

Upon the incidence of a positron on a solid surface, it will either backscatter or will implant into the material.

In the latter case, the positron will interact with matter by undergoing thermalisation, followed by diffusion and, in materials with a lower electronic density, possibly formation of positronium (Ps) atoms. Furthermore, the positron or Ps atoms, while diffusing within the material's atomic lattice, might suffer trapping at specific sites and finally annihilate with an electron of the medium.

Positronium formation After the processes of thermalisation and diffusion, the formation of positronium atoms can take place, but only in materials with a low electron density, such as polymers or insulators, where a fraction of the injected positrons, typically 10 to 50%, will form Ps atoms before they have the chance to annihilate with an electron in the surroundings. A positronium atom is created when a positron captures a host electron and a neutral but unstable bound state of the positron-electron pair is created, as an analogue of the hydrogen atom, but with the proton replaced by a positron, whose instability will inevitably lead to its decay through a positron-electron annihilation. The positronium in the ground state can exist in two different configurations depending on the alignment of the spins of the positron and the electron. On one hand, it can exist as a singlet state, also called para-positronium (p-Ps), which corresponds to 1/4 of the Ps atoms formed and where the spins of the electron and positron are in opposite directions. The p-Ps state, which has a mean characteristic lifetime, from creation into eventual self-annihilation, of 125 ps in vacuum, decays primarily through the emission of two back-to-back 511 keV γ-rays. On the other hand, Ps atoms can exist as a triplet state, known as ortho-positronium or o-Ps, which corresponds to the remaining Ps atoms formed and where the spins of the electron and positron are in the same direction. The o-Ps state, with a longer mean characteristic lifetime of 142 ns in vacuum, typically decays into three γ-rays.

Trapping In materials such as metals and semiconductors, with a high density of free electrons, containing lattice imperfections, such as defects or dislocations, both atoms and electrons may either be missing or their density may be locally reduced at these flaws. The combined effect of the reduction of the Coulomb repulsion by the positively-charged ion cores and the redistribution of electrons causes a deep negative electrostatic potential trap at these defects. Therefore, positrons see these locations as strongly attractive centres in the material and thus are very likely to get trapped in one of these sites. Conversely, in materials, such as polymers and insulators, with a low electron density, there is usually an abundance of areas of lower nuclear and electron charge density, such as pores or vacancies. The reduced dielectric response of the medium in such locations leads to a higher binding energy for both positrons and Ps atoms and thus near these defects they are pushed into them.

Annihilation In their free state, positrons will annihilate with either a valence electron of an atom or a free electron. In annihilation, the particles collide, disappear and convert their mass entirely into electromagnetic energy, in the form of gamma photons. In the centre-of-mass frame, the photons' total energy is equal to $E = 2m_e c^2 = 1022$ keV, where m_e is the rest mass of the electron (or positron). This annihilation almost always yields two γ-rays of an equal energy of 511 keV, travelling in opposite directions. All positrons injected into a material which annihilate from this free state, tend to do so with approximately the same lifetime, which is characteristic of the material as it is proportional to the effective electron density sampled by the positrons. Similarly, positrons trapped either in defects in high electron density materials or voids in low electron density ones will also annihilate according to this scheme, but this time with an electron they may encounter on one of their many collisions with the defect's or void's walls when trapped inside their potential. Since the local electron density is lower, it is expected that positrons reside here for longer periods of time, given that they have increased difficulty in finding an electron to annihilate themselves with. For a given type of material, the larger the defect size, the longer positrons can reside in it and vice-versa.

Unlike positrons, free Ps atoms, while diffusing through the medium can suffer self-annihilation. This annihilation mechanism has a very well defined associated lifetime for p-Ps and o-Ps atoms as they annihilate with their intrinsic self-annihilation lifetime, not the one for vacuum, but instead with a characteristic one specific for the material in which they were formed. Finally, when Ps atoms are trapped inside the potential well of voids within materials with a low electron density they will move through the void, colliding with its walls, until they find, in one of these collisions, a bound molecular electron with opposite spin to that of the positron, at which point a so-called "pick-off" annihilation occurs. This is an interaction by which the positron in the Ps atom does not annihilate with its bound electron, but instead with this found electron in a 2 γ-ray emission process. Despite the fact that this process is possible for both p-Ps and o-Ps atoms, it is not as relevant for the p-Ps because it tends to self-annihilate before it has a chance to find an electron of opposite spin in the walls of the free volume or indeed be trapped inside it. With each bounce on the wall, there is a certain probability that the o-Ps annihilates with a molecular electron, which is strongly dependent on the void size, given that in smaller voids more Ps-wall collisions will take place, leading to a faster "pick-off" annihilation. This results in that the lifetime of the specimens in this trapped state increases systematically with increasing size of the free volume.

The possible annihilation processes, and respective characteristic time scales are summarised in *Figure 1*. The trapped states' annihilations have a characteristic time scale that is dependent on the morphology and structure of the free volumes where the annihilations take place. Hence, the existence of these states and their lifetime determination through the PALS technique provides valuable information about the material with regards to

its internal free volumes as the positron or Ps lifetime reflects their size, respectively, for when metals and semiconductors are under analysis or for when polymers and insulators are being studied. Moreover, for the latter case, the trapped o-Ps state is the one that is more likely to take place and therefore is the one that plays the key role in providing the relevant information concerning the material's free volume structure.

High electron density materials

Low electron density materials

Positron state	Annihilation process	Characteristic time scale
Free e^+	2γ self-annihilation	0.1 – 0.4 ns
Trapped e^+	2γ self-annihilation	0.2 – 0.5 ns
Free p-Ps	2γ self-annihilation	0.125 ns in vacuum
Trapped p-Ps	2γ pick-off annihilation	up to dozens of ps
Free o-Ps	3γ self-annihilation	142 ns in vacuum
Trapped o-Ps	2γ pick-off annihilation	up to dozens of ns

Dependent on the free volume structure

FIG. 1. Characteristic time scales of the different positron annihilation processes. Table containing data from [1].

III. MATERIALS AND METHODS

PALS measures the lifetime of positrons as the time interval between their implantation into the analysed material and the emission of a γ-ray resultant from their annihilation through one of the many discussed processes. After a reasonable amount, between 10^5 and 10^6, of these events has been detected, a lifetime spectrum is obtained, representing the number of annihilation events of the implanted positrons versus their lifetime. This spectrum contains several lifetime components associated with different annihilation processes and some even depending on the existence and size of free volumes inside the material, due to the fact that each annihilation process has its own characteristic time signature and the fact that positrons or Ps atoms trapped inside free volumes will reside there for different time periods, depending on their size. It is with the decomposition of the acquired spectrum into these individual lifetime components and corresponding intensities that is possible to extract information regarding the size, concentration and nature of the free volumes in the probed material. Hence, in order to conduct a PALS analysis three aspects are essential: a source of positrons; an experimental setup, where the time of each event is detected and recorded; and an analysis method and software that enable the decomposition of the acquired spectrum into the individual time components and the correlation of these results with information regarding the free volume structure of the material under study.

A. Positron source

There are two methods of implanting positrons onto a sample under study and the choice of which method to employ relies on the type of study that is desired. These consist of a positron emitting radioactive source that suffers β^+ decay and emits positrons with a continuous spectrum of energies or a linear accelerator that produces positron beams of variable and well defined energy. For this work, a positron emitting radioactive source, indeed a much more straightforward technique, was preferred, with the ^{22}Na radioactive isotope selected for this purpose. This radioisotope is the most frequently employed in PALS analysis due its many advantages: the source is of simple production, handling and substitution and the isotope has a long half-life of 2.6 years suitable for the intended studies, given that it is ensured that not only does the source's activity remains nearly constant for the duration of a data acquisition run but also that the same source can be used for multiple runs. The ^{22}Na decay scheme is represented in *Figure 2*. As shown, the relevant decay is that to the 1274 keV excited state of ^{22}Ne through β^+ decay, which is accompanied by the emission of positrons with a continuous energy spectrum with an end-point energy of 545 keV. This high positron yield is another essential attribute of this radioisotope that makes it particularly fitting for the production of positrons for a PALS experiment.

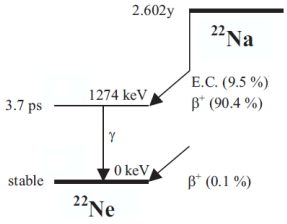

FIG. 2. Decay scheme of ^{22}Na. Adapted from [1]

B. Experimental setup

The experimental setup used in this work comprises: a detection system, for the detection of the implantation of a positron into the material and its ensuing annihilation; and a subsequent set of analog electronic modules, where the signals provided by the scintillators are processed to determine and register the value of the positron lifetime. The spectrometer used in this work is schematically represented in *Figure 3*.

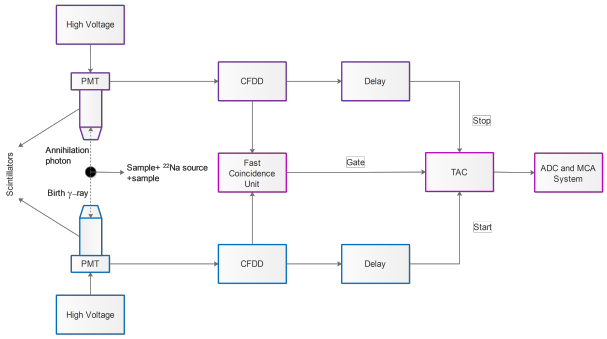

FIG. 3. Block diagram of the PALS experimental setup used in this work.

Detection system The detection system is thus intended to register the arrival times of two signals, one marking the implantation of the positron into the material and the other its annihilation. These signals are known, respectively, as start and stop signals and the time difference between the two establishes the positron lifetime. Since the half-life of the excited state of ^{22}Ne is only about 3.7 picoseconds, succeeded by the prompt emission of a 1274 keV γ-ray as the isotope transitions

to its ground state, both positron and 1274 keV γ-ray emissions can be considered simultaneous and the detection of this γ-ray is taken as the start signal. The stop signal, on the other hand, is considered as the detection of a 511 keV γ-ray resultant from a 2 γ-ray positron annihilation process in the material. For the detection of these signals to be possible, a sandwich composed of the ^{22}Na radioactive source and two pieces of the sample under analysis placed in close contact on either side of it, is positioned at an equal distance between the two scintillators, which in turn are facing each other. In a typical PALS experimental setup, the detection of the 1274 keV and 511 keV γ-rays is achieved by using two scintillation detectors, one for each gamma ray. For this work, the detectors chosen were barium fluoride (BaF_2) crystalline scintillators, that represent a rather satisfactory compromise between efficiency and time response. Owing to the fact that scintillators produce extremely weak light pulses when bombarded with incoming charged particles or radiation, they must be coupled to a photomultiplier tube. The PMT's function is to convert these scintillations into analog, electronic pulses of a high sufficient electronic charge, whose amplitude is proportional to the energy deposited in the scintillator by the original gamma-ray and that can then be transmitted to and processed by the associated electronic modules in order to register the positrons lifetime.

Electronic modules The output pulses from each PMT are then sent to two dedicated Constant Fraction Differential Discriminators (CFDD). They are used to mark the pulses' exact arrival time, through the simultaneous generation of both a fast negative signal, containing the relevant timing information and a slow positive output. Additionally, the CFDDs have upper and lower voltage level discriminators, ensuring that the outputs are only generated if the input pulses from the photomultiplier tube fall within the preset accepted amplitude range, *i.e.* if they simultaneously exceed the lower-level threshold and do not exceed the upper-level one. In that sense, one of the CFDDs is used to generate the start signal, thereafter referred to as the start CFDD, by being set to accept only the 1274 keV γ-rays and the other, from here on referred to as the stop CFDD, is prepared to be receptive only of 511 keV photons and therefore output the stop signal. The fast timing signals generated by each CFDD are fed to the start and stop inputs of a Time-to-Amplitude Converter (TAC), but only after being passed through a RG58 cable of a length determined according to the time delay intended. Subsequently, the TAC produces an analog pulse, whose amplitude is proportional to the time difference between the arrival of the two signals. However, in such a configuration, the TAC might be flooded with a large number of signals at its start input with no corresponding stop signals, causing a considerable dead time in the TAC. In order to prevent this, the slow positive output signals from the CFDDs are led to a Fast Coincidence Unit (FC Unit), likewise connected to the TAC. This unit serves the purpose of producing a gate signal in case it detects a coincidence event of photons of proper energies within the selected time frame, in other words, if a start and stop signal reach the unit within a specified time interval of each other. Only in the presence of this gate signal at the gate input of the TAC does the latter generate its output pulse, reason why a time delay is imposed to both the start and stop signals generated by the CFDDs, so as to compensate for the time required by the FC unit to process incoming signals and transmit a gate one. Finally, the TAC pulses are digitised by an Analogue-to-Digital Converter (ADC) and conducted to a Multi-Channel Analyser (MCA), where each event is stored in a histogram as one count in the channel that corresponds to that particular signal amplitude. During a run of data acquisition, multiple events are recorded in this histogram that constitutes the positron annihilation lifetime spectrum and represents the number of annihilation events of the implanted positrons versus their lifetime, in other words, the number of positrons that lived for a particular time span.

Our complete PALS experimental setup is shown in *Figure 4*.

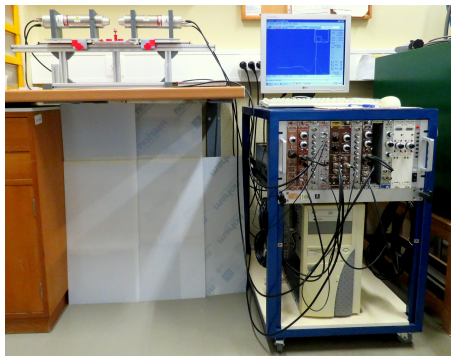

FIG. 4. Experimental setup employed in this work.

C. Positron lifetime spectra analysis

A PALS analysis is then concluded using a software to deconvolute the acquired positron lifetime spectrum into recognisable and useful parameters such as positron lifetimes and intensities of the annihilation channels in order to correlate them with important aspects of the free volume structure of the material analysed, such as free volumes' size, size distribution and concentration.

Multiexponential model As a means to fully understand the role and functionalities of the deconvolution software, it is perhaps better to start by discussing the description of the positron lifetime spectrum according to the Multiexponential Model. As we have seen, a positron lifetime spectrum consists of a record of the lifetime of each positron that has annihilated in the sample under study from one of the multiple possible states. Each of these states has its own characteristic positron lifetime as well as its own occurrence frequency, that determines the prevalence of a particular annihilation channel relative to the others. As a result, to each state is associated a positron lifetime function or lifetime component

that represents the respective annihilation process and is characterised by both a lifetime and an relative intensity. According to the multiexponential model, each of these positron lifetime functions can be described as a decreasing exponential decay function. Therefore, an ideal positron lifetime spectrum is the result of the sum of n exponential decay components, each with its own lifetime and relative intensity, with n being the number of different states from which positrons have annihilated from when passing through the sample under study. Hence, an ideal positron lifetime spectrum is described by the following equation, where $\sum_{i=1}^{n} I_i = 1$, N(t) the time density of counts in the spectrum and τ_i and I_i are, respectively, the lifetime and relative intensity of the i^{th} component:

$$N(t) = \sum_{i=1}^{n} \frac{I_i}{\tau_i} \exp\left(-\frac{t}{\tau_i}\right) \quad (1)$$

However, the shape of a real positron lifetime spectrum is modified by a flat random background that accumulates under the spectrum and also by the finite time resolution of the detectors and associated electronics. The influence of the flat background is accounted for by simply adding its value, B, to the ideal spectrum equation. The influence of the time resolution, on the other hand, is a bit more complex to account for. The time resolution function, R(t), describes the response of the set of detectors and electronic modules to prompt coincidences. If it was an ideal set, when the detected lifetime is zero, a delta function would appear in the lifetime spectrum. In reality, the time spectrometer generates a prompt peak in the lifetime spectrum, *i.e.* the time resolution function, that is described as a gaussian function with exponential tails on both sides, a function known as Exponential Sided Gaussian (ESG) [2]. In practice, the time resolution is measured with the aid of a ^{60}Co radioactive source, whose decay scheme is represented in *Figure 5*.

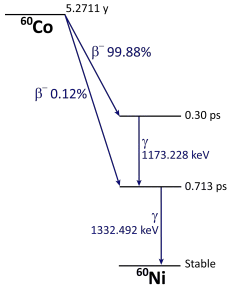

FIG. 5. Decay scheme of ^{60}Co.

The deexcitation of both excited states of ^{60}Ni as the isotope transitions to its ground state results in the emission of a 1173 keV γ-ray, followed by a second 1332 keV γ-ray separated only by 0.713 ps. As these two γ-rays are emitted virtually in prompt coincidence, their detection by the PALS system, with the first emitted one taken as the start signal and the second as the stop signal, due to the system's limited resolving capability, should produce a peak resembling a gaussian function, whose description as an ESG function conveys the overall time resolution function of the system. The real non-ideal positron lifetime spectrum, C(t), is thus the result of the convolution of such function with the sum of the theoretical description of the ideal spectrum and the background.

Analysis software The role of the analysis software is then to extract the physically meaningful parameters of the positron lifetime functions, resolution and background that compose the acquired experimental spectrum by fitting it into the multiexponential model description. In our work, PALSfit3 [3] was selected as our analysis software, mainly due to its rather straightforward approach and extremely reliable analysis procedure. PALSfit was developed by the Risø Campus of Technical University of Denmark and is a mature program that has been thoroughly tested and upgraded over the years. The program is divided into two modules: ResolutionFit and PositronFit. In the ResolutionFit module, the appropriate description of the time resolution function of the PALS system is extracted by fitting an experimental spectrum to the multiexponential model. The description obtained for the time resolution function can subsequently be imported to PositronFit where the same model is fitted to the experimental spectra. But now, because the time resolution function is already determined and fixed, the lifetimes and respective intensities of the lifetime components can be estimated.

D. Analysed samples

For the ensuing optimisation of the PALS spectrometer, lifetime spectra of materials with well known behaviour have to be acquired with the experimental setup and the positron lifetimes found from their analysis have to be compared with the values reported in literature. For this purpose, the most commonly examined materials tend to be pure metals and semiconductors as they tend to exhibit only one short lifetime component in their spectrum, associated with the positron annihilations in the bulk of the material, which, therefore, greatly facilitates a comparison of the results obtained with the values found in literature. It is also important for the scope of this work to study polymeric reference materials, given that after the optimisation of the spectrometer, it is intended to be applied mainly to the study of polymeric materials developed by the research group. In summary, three types of samples are analysed in the course of this work: metallic and semiconductor reference materials; polymeric reference materials; and finally radiation processed polymer-based materials, developed by GREI.

The metallic and semiconductor reference samples chosen were high purity polycrystalline copper (Cu) samples, high purity polycrystalline nickel (Ni) samples and electronic-grade silicon samples. Although it could be expected that high purity metal foils present a single positron lifetime component with a value close to the ones reported in literature, the reality is that the manufacturing processes involved in their production typically create defects and atom dislocations in the samples, therefore generating trapping sites where positrons might

get trapped and consequently annihilate with a different lifetime from that of free positrons. However, since a single lifetime for the metals is desired, a commonly adopted way in the PALS community to do so this is by reducing the defect concentration to a such a degree that is below the PALS technique sensitivity, which is achieved by making the acquired samples undergo an annealing process. As a single lifetime component with a similar value to the ones presented in the references was also expected in our case, it was decided to make the copper and nickel samples undergo an annealing process. For the polymeric reference samples, Polytetrafluoroethylene, also referred to as Teflon® (commercial brand name) and Polycarbonate (Bisphenol A) samples were selected.

Finally, four polymeric samples developed by the research group were studied. Two of them consisted of graft copolymer films of PE-g-HEMA (Polyethylene-grafted-Hydroxyethyl methacrylate). One of them, Sample 1, was a PE-g-HEMA film with 403% of graft, prepared by gamma irradiation, with a total dose of 9 kGy and at a rate of 0.3 kGy/h, in the absence of oxygen. The other one, Sample 2, was a PE-g-HEMA film with 158% of graft, also prepared by gamma irradiation in the absence of oxygen with a total dose of 10.5 kGy and at a similar dose rate. The remaining samples consisted of Chitosan/PVA based membranes. While one, Sample 3, was a Chitosan (Medium Molecular Weight) 2% / Polyvinyl alcohol 5% (Weight by Volume - W/V) membrane, the other, Sample 4 hereinafter, was a Chitosan (Medium Molecular Weigh) 2% / PVA 5% (W/V) / Gelatin 2% membrane, both prepared by gamma irradiation in the absence of oxygen, with a total dose of 10 kGy.

IV. OPTIMISATION OF THE PALS SETUP

The optimisation of the experimental setup concerned the proper definition of the operating parameters of the detectors, their coupled photomultiplier tubes and associated electronic modules, which was critical for two reasons. The first related to the zero channel drift observed in the lifetime spectra. The zero channel corresponds to the bin in the lifetime or the time resolution histograms with the maximum number of counts and should always be the same throughout a data acquisition run. However, it was verified that even maintaining the exact same working conditions, this zero channel greatly shifted between a wide range of channels, either within the same measurement or at the beginning of a new one. This shift it is of great concern as it causes an artificial broadening of the lifetime spectrum or the time resolution peak, leading to a faulty interpretation of the histogram by the fitting programs, resulting in unreliable and most likely incorrect values for the positrons' lifetime or the time resolution, respectively. The other aspect concerns the time resolution of the system, which is intended to be as small as possible, since the better the resolution is, the smaller the influence and even distortion on the acquired lifetime spectra is and the more reliable and accurate the spectra fitting and therefore the results are.

In order to minimise the effects of the zero channel drift and improve the system's time resolution, the following final working parameters of the spectrometer's components were established. Firstly, we determined that the maximum amplitude of the PMTs should be -2 V, in the presence of the ^{22}Na source, which meant adjusting the high voltage to a value of -1865 V and -1901 V, for the start and stop PMTs, respectively. Secondly, the WALK potentiometer of each CFDD was carefully regulated until the zero crossing was, as possible as can be, at the same exact time for all detected signals of all amplitudes, resulting in that the WALK voltage read 1.3 mV and -6.6 mV for the start and stop CFDDs, respectively. Furthermore, the start CFDD's window was regulated to guarantee that only the photopeak corresponding to the 1274 keV gamma-rays emitted practically simultaneously with the positrons resulting from the decay of the ^{22}Na source was detected. In turn, the stop CFFD's window was adjusted so that only the annihilation peak resulting from the detection of the 511 keV photons originated from the positron annihilations happening in the material under study was accepted. Additionally, the delay cables connecting the connectors in the front panel of the CFDDs, which are essential for the circuitry responsible for marking the exact arrival time of the input pulses, were defined to be RG58 cables 30.2 cm long, for both CFDDs. Moreover, the time range of the TAC, which consists of the maximum time interval between the arrival of the start and the stop signals at its inputs that is accepted for time conversion was selected to be 50 ns. The reason for this is that events with longer lifetime periods were not expected to arise from the study of neither our reference or polymeric samples. Finally, it was observed that the best time resolution, together with the best lifetime results for the reference samples were achieved when lifetime spectra containing 1 million counts were acquired with the detectors equally distanced 1 cm away from the source+samples sandwich.

The many calibrations and alterations performed on the experimental setup led to a final optimised acquisition system with a reduced zero channel drift and an improved time resolution. In fact, the zero channel drift was diminished from a shift of dozens of channels in a short period of time to a barely noticeable shift of only a few channels in long acquisition periods. On the other hand, the many adjustments carried out on the various components of the system, but in particular on the CFDDs, allowed the reduction of the time resolution to a very satisfactory value. To prove this, at the end of all modifications, a spectrum was acquired with the ^{60}Co source, for the determination of the final time resolutions, which was then fitted to an ESG function, with a C++ based script, containing functions from the ROOT library [4], in order to extract the corresponding FWHM value that is generally used to characterise any time resolution curve. The resulting graph showing the data acquired for the determination of the time resolution, alongside the ESG fitted function is presented in *Figure 6*.

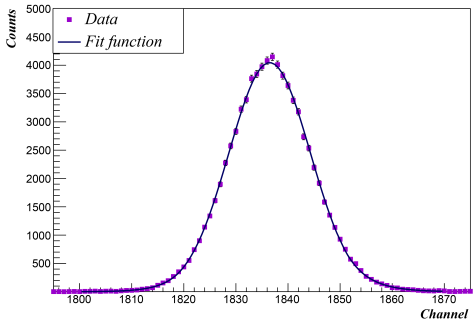

FIG. 6. Data obtained for the determination of the system's time resolution function and respective fitted ESG function.

The resultant FWHM values of the peaks were, respectively, of 164.39 ps, a more than satisfactory result, and 219.05 ps, equally admirable, in total accordance with the typical values attained with a PALS spectrometer, ranging from 180 to 250 ps.

Finally, all the optimisation work culminated in excellent results for the positron lifetimes of the reference samples, in agreement with the values reported in literature. These results will be presented in *Section V*.

V. RESULTS

For the purpose of analysing our experimental collected lifetime spectra, the PALSfit software was used, where all the parameters and settings defined were the same throughout the evaluation of all spectra, with the exception of the initial values for the lifetimes and intensities of the lifetime components, which were established individually, at the beginning of the analysis of a new spectrum as they are sample dependent. The time resolution of the system was extracted from the analysis of a reference sample spectrum, namely that of the annealed nickel samples. Nickel was preferred as it presents the shortest positron lifetime out of all the selected materials, therefore its corresponding spectrum was the simplest of all to be utilised for this purpose. The annealed samples were used because, unlike the as-received ones, their expected positron lifetime was known with a high degree of certainty. For the convergence of the fitting process, an initial guess for the FWHM value of the resolution curve had to be supplied by the user, and so, the obtained time resolution was provided, as this is indeed the time resolution with which all spectra were in fact acquired and so it is expected that the fitting software is capable of obtaining a value similar to this one. In the end, the fit provided a description of the time resolution function in the form of a gaussian function with a FWHM value of 212.5 ± 1.9 ps, a value quite close to the 219.05 ps obtained for the real time resolution. Hence, this was the time resolution description that was considered for the analysis of the remaining spectra.

When a lifetime spectrum is acquired, apart from the background radiations, the undesired annihilations happening in the surrounding environment and the effect of the spectrometer's time resolution, there is a fourth external contribution to the spectrum, known as the source correction component. This term appears due to the fact that when positrons are emitted by the radioactive source, they are required to pass through the source itself and the Kapton® HN foils that encapsulate the source, in order to reach the sample pieces under study. During this crossing, despite the tiny volume of the source's crystallites and the small thickness of the Kapton® HN foils, a non-negligible number of positrons will annihilate within this set, creating an additional lifetime component in the spectrum. The source contribution was determined with the analysis of the same annealed Ni sample spectrum, where three lifetime components were considered, with one of them associated to annihilations in the radioactive source. The lifetime result obtained for this component was 364.9 ± 5.4 ps, which is considerably close to the expected 381.34 ps, corresponding to the average value computed for the positron lifetime in Kapton® HN [5–26], which was set as the initial guess for this component. From this point onwards, an additional lifetime component accounting for annihilations in the positron source, with a fixed lifetime value of 364.9 ps, was added in the evaluation of the lifetime spectra. However, its relative intensity was kept a free parameter, since the strength of the source contribution is different for every sample as it is heavily dependent on factors such as density and atomic number of the sample under study.

A. PALS results for the reference samples

Metallic and semiconductor reference samples The first evaluated lifetime spectra were the ones collected with the as-received and annealed Ni and Cu samples and the EG-Si samples. Each spectrum was resolved into three discrete lifetime components corresponding, from shortest to longest, to: the free positrons annihilations in the bulk of the sample, characterised by the lifetime τ_{bulk} and relative intensity I_{bulk}; the source contribution, described by the lifetime τ_{source} and relative intensity I_{source}; and the positron annihilations in the surrounding environment, such as neighbouring materials or the air layers between the samples and the source and between the source+sample sandwich and the detectors, defined by the lifetime τ_{env} and relative intensity I_{env}. The lifetime spectrum acquired with the annealed Ni samples, decomposed into its constituent lifetime components by the analysis software is shown in *Figure 7*.

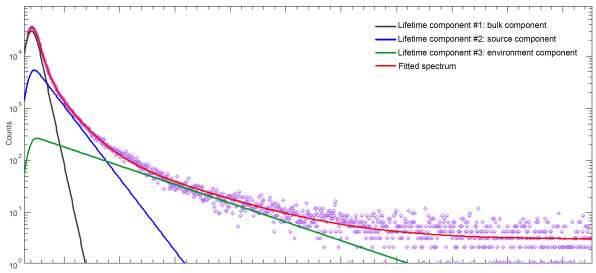

FIG. 7. Experimental lifetime spectrum acquired with the annealed Ni samples and the result of its decomposition into three lifetime components.

This is shown with the intent to demonstrate the typical fitting process and decomposition of a lifetime spectrum, which is fairly similar for all spectra, reason why the remaining analysed lifetime spectra acquired for the other materials are not presented in this document. The analysis of the spectra obtained for the metallic and semiconductor samples, as well as for all the remaining samples, resulted in reduced χ^2 values pretty close to 1, signifying pretty good fits and consequently reliable results.

The lifetime results obtained for the bulk component from the analysis of both the as-received and annealed Ni and Cu samples, as well of the EG-Si samples are displayed in *Table I*. Furthermore, the average bulk lifetime value computed with the results reported in a plethora of studies for each material and the percentage deviation of the obtained values for the annealed Ni and Cu samples and the EG-Si samples from these bulk average values are also presented.

Material	Bulk lifetime of as-received sample (ps)	Bulk lifetime of annealed sample (ps)	Average bulk lifetime from literature (ps)	Deviation from average value (%)
Ni	144.3 ± 0.9	102.3 ± 1.0	106.96 [5, 12, 14, 26–31]	4.36
Cu	147.5 ± 0.9	111.2 ± 0.7	116.19 [5, 12, 16, 20, 26–30, 32]	4.49
EG-Si	171.7 ± 1.1	-	179.33[33–35]	4.26

TABLE I. Bulk lifetimes obtained from the analysis of as-received and annealed Ni and Cu samples and EG-Si samples, compared with the respective values reported in literature.

Polymeric reference samples A study of Teflon® and Polycarbonate ensued. An effort was made to decompose each spectrum into the five expected components, which, from shortest to longest were ascribed to: a mixture of free p-Ps atoms annihilations in the bulk of the material and an unknown contribution, the source contribution of fixed lifetime, the free positrons annihilations in the bulk of the material, the trapped o-Ps atoms annihilations in the material's free volume structure and positron annihilations in the surrounding environment. However, fits containing so many free parameters were impossible to produce and instead a three component fit was achieved for each spectrum, containing solely the lifetime components corresponding to p-Ps atoms, free positrons and o-Ps atoms annihilations in the sample, respectively, with lifetimes and intensities τ_1 and I_1, τ_2 and I_2 and τ_3 and I_3. The literature reported lifetime and relative intensity values for these three components are summarised in *Table II*.

Material	τ_1 (ns)	I_1 (%)	τ_2 (ns)	I_2 (%)	τ_3 (ns)	I_3 (%)	Reference
Teflon®	0.32	72.63	0.93	11.4	3.89	15.97	[36]
	0.25	50.32	0.747	25.98	3.931	23.7	[37]
Polycarbonate	0.125	-	0.4	-	2.14	28.5	[38]
	0.22	38-49	0.5-0.62	20-31	2.03-2.13	27.5-29	[39]
	0.12-0.28	19-21	0.35-0.45	39-45	2.05-2.08	28-34	[40]
	0.19	23	0.41	46	2.05	30	[41]
	0.231	42.6	0.495	27.5	2.032	29.9	[25]
	0.242	42.8	0.47	26.8	2.014	30.5	

TABLE II. Published positron lifetime values for Teflon® and Polycarbonate.

The results obtained for the lifetimes and associated intensities of each lifetime component are, respectively, expressed in *Tables III* and *IV*.

τ_1 (ps)	I_1 (%)	τ_2 (ps)	I_2 (%)	τ_3 (ps)	I_3 (%)
207.3 ± 1.5	58.40 ± 0.42	731.3 ± 6.9	35.36 ± 0.37	3977.4 ± 63.1	6.24 ± 0.09

TABLE III. Lifetimes and respective intensities of the lifetime components resultant from the deconvolution of the lifetime spectrum acquired with the Teflon® samples.

τ_1 (ps)	I_1 (%)	τ_2 (ps)	I_2 (%)	τ_3 (ps)	I_3 (%)
208.5 ± 1.8	55.85 ± 0.48	748.8 ± 9.8	37.13 ± 0.35	2312.9 ± 45.0	7.02 ± 0.29

TABLE IV. Lifetimes and respective intensities of the lifetime components resultant from the deconvolution of the lifetime spectrum acquired with the Polycarbonate samples.

B. PALS results for the polymeric samples

Finally, the polymeric samples developed by the research group were analysed. Given the very small thickness of these samples, in order to properly acquire their lifetime spectra without an immense undesired contribution from surrounding positron annihilations, an annealed Ni sample was placed in either side of the sample+source sandwich. A reference metal with a very short lifetime component was preferred for this purpose as its contribution to the spectrum amounts solely to an extremely short extra lifetime component, unlikely to be confused with any of the polymer's lifetime components. Therefore, an additional lifetime component, corresponding to annihilations within Ni, was taken into account.

Six lifetime components were considered in each spectrum, corresponding to: free positron annihilations in the bulk of the annealed Ni samples, free p-Ps atoms annihilations in the bulk of the materials, positron annihilations in the source set, free positrons annihilations in the bulk of the material, trapped o-Ps atoms annihilations in the material's free volume structure and positron annihilations in the surrounding environment, from shortest to longest. Nonetheless, just like before, a fit with so many unconstrained parameters was not achievable. In turn, a fit considering exclusively the lifetime components of the bulk annihilations in annealed Ni, with a lifetime fixed to 102.3 ps (the value previously found for the bulk component in the annealed Ni samples), and the p-Ps atoms, free positrons and o-Ps atoms annihilations in the polymeric sample, respectively with lifetimes and intensities τ_1 and I_1, τ_2 and I_2, τ_3 and I_3 and τ_4 and I_4, was considered. The final results for the lifetimes and associated intensities associated with annihilations in the samples, obtained for Samples 1, 2, 3 and 4 are summarised in *Table V*.

	τ_2 (ps)	I_2 (%)	τ_3 (ps)	I_3 (%)	τ_4 (ps)	I_4 (%)
1	253.8 ± 8.8	30.81 ± 0.70	669.7 ± 19.9	19.40 ± 0.92	2269.5 ± 110.6	1.90 ± 0.18
2	264.7 ± 9.6	26.77 ± 0.67	682.9 ± 25.3	14.64 ± 0.89	2368.2 ± 138.6	1.50 ± 0.17
3	226.5 ± 7.7	36.60 ± 0.80	631.5 ± 14.6	26.42 ± 0.89	1974.6 ± 119.3	1.69 ± 0.23
4	221.6 ± 7.9	35.60 ± 0.84	622.7 ± 14.3	25.64 ± 0.87	1992.4 ± 116.6	1.65 ± 0.21

TABLE V. Lifetimes and respective intensities of the lifetime components resultant from the deconvolution of the lifetime spectrum acquired with each polymeric sample, with τ_1 fixed at 102.3 ps during the fitting process.

1. *Pore size determination*

Since τ_4 is associated with o-Ps annihilations occurring inside the free volume structure within the samples, it was then desired to determine the size of the pores where these annihilations had taken place. In order to do so, theoretical models have been designed to correlate their size with the observed lifetime of the o-Ps atoms.

Tao-Eldrup Model The original model for free volume size estimation with PALS parameters is the Tao-Eldrup (TE) Model [42, 43]. The model regards the o-Ps atom as a single quantum particle and approximates the free volumes as infinitely deep spherically potential wells, that confine the o-Ps to the ground state. They are described by the quantity R + ΔR, where R is the radius of the electron-free infinite potential barrier region, where the potential is zero and the o-Ps lifetime is assumed to be that of vacuum and ΔR is the depth of the potential barrier, that is the thickness of the virtual electron layer assumed to be the cavity walls where the electron density is constant and with which the o-Ps wave function overlaps and where eventually annihilates by pick-off annihilation. Furthermore, the TE Model ignores the o-Ps vacuum self-annihilation rate in the central portion of the pore and the overall annihilation rate of the o-Ps atom, λ_{TE}, is solely the pick-off annihilation rate due to the interactions with electrons in the walls of the free volume, resulting in:

$$\lambda_{TE} = 2\left(1 - \frac{R}{R+\Delta R} + \frac{1}{2\pi} sin\left(\frac{2\pi R}{R+\Delta R}\right)\right) \quad (2)$$

The most commonly used value for ΔR in polymers, determined empirically by fitting the above equation to experimental data is 0.1656 nm.

The Tokyo Model Despite giving quite accurate results for the radius of free volumes, the Tao-Eldrup Model is not suitable for pores greater than 1 nm. An extension of the Tao-Eldrup Model to the analysis of materials with larger free volumes, the Tokyo Model was suggested [44]. While maintaining the presumed spherical geometry of the free volumes, the model assumes that, inside a pore, the o-Ps atom has a natural annihilation rate equal to its vacuum annihilation rate, λ_{o-Ps}, plus an additional term whose value depends on whether the radius of the pore is smaller or larger than a critical radius R_a. This results in the following total annihilation rate:

$$\lambda_{Tokyo}(R) = \begin{cases} \lambda_{TE}(R) + \lambda_{o-Ps} & R < R_a \\ \lambda_{TE}(R_a)\left(1 - \left(\frac{R-R_a}{R+\Delta R}\right)^b\right) + \lambda_T & R \geq R_a \end{cases} \quad (3)$$

The values of the two free parameters were adjusted by fitting experimental data to the model and have been determined as $R_a = 0.8$ nm and b = 0.55 [44].

The equations presented relate the rate of o-Ps annihilations with the size of pores where this annihilation has taken place. However, by inverting these equations, according to the relation $\lambda = 1/\tau$, a straightforward correlation between the lifetime, τ, of o-Ps atoms obtained from the fitting procedure, given in ns, and the radius of the free volumes is achieved. These relations were then applied to the o-Ps lifetimes attained by the fitting of the polymeric samples' experimental lifetime spectra, through a Mathematica code script, developed for the effect. The results obtained are expressed in *Table VI*, for each sample and according to each model, in terms of both radius and mean free path.

Samples	Radius (nm)		Mean free path (nm)	
	TE Model	Tokyo Model	TE Model	Tokyo Model
1	0.309	0.312	0.412	0.416
2	0.317	0.320	0.423	0.427
3	0.283	0.286	0.377	0.381
4	0.285	0.287	0.380	0.383

TABLE VI. Radius and mean free path values estimated for the free volumes inside each polymeric sample.

VI. CONCLUSIONS

At the end of our work, the calibration steps taken, the alterations performed and the performance tests carried out on the experimental setup resulted in a stable spectrometer capable of producing lifetime spectra with a time resolution on par with some of the best resolution values reported in literature.

The results obtained from the analysis of the lifetime spectra acquired with the annealed Ni, annealed Cu and EG- Si reference samples are in excellent agreement with the average of previously published literature values. For the Teflon® and Polycarbonate samples, the agreement with literature is not so evident but is nevertheless satisfactory. This outcome was expected as being polymers, slight deviations in characteristics, such as density or internal free volume structure, from those of the samples considered in different published studies can induce an entirely distinct behaviour of positrons inside them and consequently different obtained positron lifetimes. From the PALS measurements with our own polymeric samples, lifetime and subsequently free volumes' size values within the reasonable and expected range were achieved. The spectrometer was also effective in discerning the different compositions of the samples and the distinct production conditions and parameters involved in their development, by generating different free volumes' sizes for all of them. However, a deeper understanding of the mechanisms involved in the creation of these free volumes and of the implications of this free volume structure on the samples' performance for their intended purposes requires further measurements and studies, not only with PALS, but also with complementary probing techniques.

From the present observations, it could be concluded that, in the end, we were capable of attaining an optimised PALS spectrometer, a set of acquisition and analysis tools and a broad knowledge of the PALS technique, that together will allow GREI to perform consistently accurate PALS measurements that will shed some light on the free volume structure of the macromolecular materials developed by the group and, more broadly, on their overall behaviour, attributes and performance. With this PALS setup, apart from the study of the multiple macromulecular materials developed by the research group, it would also be interesting to apply it to both an interlaboratory study and a study employing other probing

techniques, not only as an additional step to validate the work here performed and to attest the quality of our spectrometer but also to contribute for the standardisation of certain aspects of the PALS technique. We have seen, in the course of this work, that both the occasional omission, in certain published studies, of the acquisition and analysis procedures carried out and the lack of a widely accepted way to perform these procedures greatly impairs the work of researchers and thus it would be extremely important that studies aimed at contributing to an even greater success of the PALS technique could be carried out with this setup.

[1] I. Procházka, Materials Structure **8**, 55 (2001).
[2] S. Das, arXiv: High Energy Physics - Experiment (2016).
[3] J. Olsen, P. Kirkegaard, N. Pedersen, and M. Eldrup, Physica Status Solidi. C: Current Topics in Solid State Physics **4**, 4004 (2007).
[4] Root, `https://root.cern/` (2021).
[5] Ortec, Educational Experiments **27**, https://www.ortec-online.com/service-and-support/library/educational-experiments (2008).
[6] J. Kansy and T. Suzuki, Radiation Physics and Chemistry **76**, 291 (2007), proceedings of the 8th International Workshop on Positron and Positronium Chemistry.
[7] J. Kansy, Acta Physica Polonica A **113**, 1397 (2008).
[8] Y. Yu, *Positron annihilation lifetime spectroscopy - studies of amorphous and crystalline molecular materials*, Ph.D. thesis, Martin-Luther-Universität Halle-Wittenberg (2011).
[9] C. Dauwe, B. Waeyenberge, G. Consolati, J. Kansy, D. Segers, T. Van Hoecke, and F. Du Prez, Materials Science Forum **255-257**, 62 (1997).
[10] K. Płotkowski, T. J. Panek, and J. Kansy, Il Nuovo Cimento D **10**, 933 (1988).
[11] G. S. Kanda, L. Ravelli, B. Löwe, W. Egger, and D. J. Keeble, Journal of Physics D Applied Physics **49**, 025305 (2016).
[12] G. Kanda, Positron annihilation lifetime spectroscopy methodology and application to perovskite oxide materials (2015), thesis.
[13] G. Kanda and D. Keeble, Nuclear Instruments and Methods in Physics Research Section A Accelerators Spectrometers Detectors and Associated Equipment **808**, 54 (2016).
[14] S. McGuire and D. J. Keeble, Journal of Applied Physics **100**, 103504 (2006).
[15] M. A. Söylemez and O. Güven, Journal of Molecular Recognition **31**, e2676 (2018).
[16] N. Djourelov and M. Misheva, Journal of Physics: Condensed Matter **8**, 2081 (1996).
[17] S. K. Sharma, K. Sudarshan, M. Sahu, and P. K. Pujari, RSC Adv. **6**, 67997 (2016).
[18] R. A. Mackie, S. Singh, J. Laverock, S. B. Dugdale, and D. J. Keeble, Physical Review B **79**, http://dx.doi.org/10.1103/PhysRevB.79.014102 (2009).
[19] K. Dulski, Assembly and calibration of apparatus for positron annihilation lifetime spectroscopy (2016), thesis.
[20] A. Karbowski, J. Fidelus, and G. Karwasz, Materials Science Forum **666**, 155 (2010).
[21] D. Petschke and T. E. Staab, SoftwareX **10**, 100261 (2019).
[22] A. Saoucha, Journal of Applied Physics **85**, 1802 (1999).
[23] D. Petschke, R. Helm, and T. Staab, Data in Brief **22**, 16 (2019).
[24] J. M. M. Luís, *Espectroscopia de tempos de vida de aniquilação do positrão no estudo dos processos de relaxação e absorção de humidade num polímero comercial*, Master's thesis, Universidade de Coimbra (2010), thesis.
[25] G. Dlubek, A. Clarke, H. Fretwell, S. Dugdale, and M. Alam, Journal of Radioanalytical and Nuclear Chemistry **211**, 69 (1996).
[26] B. M. Wieland, *Construction and Testing of a Positron Annihilation Lifetime Spectrometer*, Master's thesis, Idaho State University (2012), thesis.
[27] T. Staab, B. Somieski, and R. Krause-Rehberg, Nuclear Instruments and Methods in Physics Research Section A: Accelerators, Spectrometers, Detectors and Associated Equipment **381**, 141 (1996).
[28] J. Campillo Robles and F. Plazaola, Defect and Diffusion Forum **213-215**, 141 (2003).
[29] J. Kansy, Nuclear Instruments and Methods in Physics Research Section A: Accelerators, Spectrometers, Detectors and Associated Equipment **374**, 235 (1996).
[30] D. Giebel and J. Kansy, Physics Procedia **35**, 122 (2012), positron Studies of Defects 2011.
[31] S. McGuire and D. Keeble, Journal of Physics D **39**, 3388 (2006).
[32] I. Bishay, E. H. Aly, and F. Saadallah, Materials Science and Engineering: A **527**, 3893 (2010).
[33] C. Y. Lee, Applied Science and Convergence Technology **25**, 85 (2016).
[34] D. T. Britton, P. Willutzki, T. E. Jackman, and P. Mascher, Journal of Physics: Condensed Matter **4**, 8511 (1992).
[35] S. C. Sharma, N. Hozhabri, R. G. Hyer, T. Hossain, S. Kim, F. O. Meyer, M. Pas, and A. E. Stephens, MRS Proceedings **262**, 45 (1992).
[36] S. J. Tao and J. H. Green, Proceedings of the Physical Society **85**, 463 (1965).
[37] P. Kindl, W. Puff, and H. Sormann, physica status solidi (a) **58**, 489 (1980).
[38] D. Cangialosi, H. Schut, A. van Veen, and S. J. Picken, Macromolecules **36**, 142 (2003).
[39] J. E. Kluin, Z. Yu, S. Vleeshouwers, J. D. McGervey, A. M. Jamieson, and R. Simha, Macromolecules **25**, 5089 (1992).
[40] J. Kluin, Z. Yu, S. Vleeshouwers, J. McGervey, A. Jamieson, R. Simha, and K. Sommer, Macromolecules **26**, 1853 (1993).
[41] J. Bohlen and R. Kirchheim, Macromolecules **34**, 4210 (2001).
[42] S. J. Tao, The Journal of Chemical Physics **56**, 5499 (1972).
[43] M. Eldrup, D. Lightbody, and J. Sherwood, Chemical Physics **63**, 51 (1981).
[44] K. Ito, H. Nakanishi, and Y. Ujihira, The Journal of Physical Chemistry B **103**, 4555 (1999).